Neural network-based robust finite-time attitude stabilization for rigid spacecraft under angular velocity constraint

Bo Yu[1] · Haibo Du[1,2] · Lijian Ding[1] · Di Wu[3] · Hua Li[1]

Abstract

In this paper, the problem of attitude stabilization control of spacecraft under angular velocity constraint is investigated. A state-constrained finite-time attitude control scheme is designed by making full use of the model feature of the quaternion. Based on the homogeneous domination approach, the finite-time stability of the closed-loop system is proved. It proves that the angular velocity can be constrained within the limited range at any time. For the attitude loop dynamics subsystem with external disturbances, based on a radial basis function neural network, an integral terminal sliding mode controller is proposed. Finally, the validity and advantages of the proposed control scheme are demonstrated in the simulation section compared with the other two control methods.

Keywords Attitude control · State constraint · Finite-time control · RBF neural network

1 Introduction

The attitude control for a high nonlinear rigid spacecraft is a classical nonlinear control problem [1–3]. Attitude control mainly includes attitude stabilization control and attitude tracking control. Here, this note focuses on the problem of attitude stabilization control. In recent decades, in order to solve attitude stabilization control problem more effectively, a variety of control methods have been proposed, such as optimal control [4, 5], adaptive control [6, 7], backstepping control [8–10], and sliding mode control [11–18]. In [4], the inverse optimal control method was employed, and bypassing the task of solving the Hamilton-Jacobi equation obtains a meaningful cost functional optimal controller. The work [7] developed an adaptive controller for attitude stabilization of a rigid spacecraft with model uncertainties, external disturbances. In [11], a discrete-time super-twisting-like control scheme based on the sliding-mode control technique for robotic fishes was proposed, aiming at improving steering performance.

However, note that all above control schemes can only produce exponential convergence with infinite convergence time at most. Obviously, it would make sense if we could achieve a faster convergence speed in the control process [19, 20]. The control problem of attitude stabilization with finite convergence time has aroused wide attention [21–23]. Besides faster convergence rate, the control method has better robustness and disturbance rejection performance [24–29]. As a consequence, the results of finite-time control were applied to spacecraft attitude stabilization. In [30], two sliding mode controllers were employed to force that the state variables of the closed-loop

✉ Haibo Du
haibo.du@hfut.edu.cn

1   School of Electrical Engineering and Automation, Hefei University of Technology, Hefei 230009, People's Republic of China

2   Engineering Technology search Center of Industrial Automation, Hefei 230009, Anhui Province, People's Republic of China

3   School of Automation, Southeast University, Nanjing 210096, People's Republic of China

system will converge to the origin in a finite time. Based on homogeneous method and switching method, a global saturated finite-time control method was developed in this work [31].

It is worth mentioning that angular velocity is necessary for attitude stabilization control of spacecraft. In practice, the value of angular velocity cannot be arbitrarily changed. Saturation limits for low rate gyro and task specifications requirement are usually caused angular rate constraint. An example is the X-ray timing probe spacecraft, which needs to maneuver within the saturation limit of the rate gyro [32]. In industrial applications, the performance of airborne equipment is seriously affected by the excessive angular velocity. Therefore, it is valuable to study the attitude control algorithm under the constrained angular velocity of spacecraft.

In recent years, some control strategies have been presented to discuss the problem of angular velocity constraint in control domain. In the work [33], on the basis of parameterized attitude constraint region of unit quaternion, a global minimum quadratic potential function was established. And another logarithmic potential function was designed to limit the angular velocity. By using these two potential functions and sliding mode control technique, a nonlinear attitude control law was obtained to ensure the stability of closed-loop system with external disturbance and attitude and angular velocity constraints. In [34], a smooth adaptive fault-tolerant constrained controller was given which can guarantee the uniformly bounded stability of the closed-loop system. This paper [35] utilizes the barrier Lyapunov function in the analysis of the Lyapunov direct method, and the constrained behavior of the system is provided in which the rotor speed, its variation, and generated power remain in the desired bounds. The work [36] is based on the direct Lyapunov method, which by use of the Nussbaum-type function provides an adaptive control scheme that can handle the effect of unknown control direction.

Different from the existing results of [33–36], this paper considers not only attitude stabilization control of spacecraft under angular velocity constraint but also disturbance rejection control. The main difficulties lie in two aspects: (1) How to employ the model structure feature to design a state-constrained finite-time attitude control scheme. (2) How to employ RBF neural network and design a finite-time attitude controller for the attitude loop dynamics subsystem with external disturbances.

The main contributions of this paper are three aspects. (1) Compared with the existing control methods for quadrotor aircraft, the proposed control algorithm in this paper not only guarantees that the attitude stabilization in a finite time but also in the design process the angular velocity constraint is under consideration. (2) Compared with the

other finite-time control algorithms, the proposed finite-time control algorithm in this paper is mainly based on the homogeneous system theory rather than the back-stepping design. As a result, the new control algorithm has a simpler structure, which implies that it is easy to design and adjust the control parameters. (3) In addition, compared with other finite-time control algorithms, the finite-time control algorithm proposed in this paper proposes an integral terminal sliding mode controller based on RBF neural network for attitude loop dynamics subsystem with external disturbance, which effectively improves the ability of disturbance rejection.

In this paper, a finite-time stability control algorithm based on quaternion is proposed for the rigid spacecraft attitude system with angular velocity constraint. The new idea is to employ the state-dependent time-varying gain by replacing the constant gain in the traditional finite-time attitude controller. However, the resulting closed-loop system is a time-varying system that makes finite-time stability analysis challenging. In order to overcome the technical problem of finite-time stability of time-varying nonlinear closed-loop system, the whole closed-loop system is proved to be stable in a finite time by employing the idea of homogeneous domination. Based on the proposed control strategy, the spacecraft attitude can converge to the equilibrium point in a finite time and the angular velocity cannot exceed the constraint region. In order to investigate the finite-time attitude stabilization control in the presence of external disturbances, the RBF neural network algorithm is used to estimate the uncertainties of the system and an integral terminal sliding mode controller is designed. At the end, some simulation results are shown to verify the effectiveness and availability of the theoretical results.

2 Problem description

2.1 Notations

Making the equation clear in concept, denote $\text{sig}^\alpha(x) = \text{sign}(x)|x|^\alpha$, where $\alpha \geq 0, x \in \mathbb{R}$, $\text{sign}(\cdot)$ is the standard sign function.

2.2 Spacecraft attitude kinematics and dynamics

To describe the space rotation orientation of the spacecraft, the unit quaternion is employed in this paper. Specifically speaking, define Φ as the principal angle and

$$e = [e_1, e_2, e_3]^T$$

represents the principal axis associated with Euler's

theorem, where $e^T e = 1$. The quaternion representation can be described as

$$q_0 = \cos\frac{\Phi}{2}, q_v = [q_{v,1}, q_{v,2}, q_{v,3}]^T = e\sin\frac{\Phi}{2}, \tag{1}$$

which satisfies that

$$q_0^2 + q_v^T q_v = 1. \tag{2}$$

By [37], we know the kinematic equation of spacecraft attitude is

$$\dot{q} = \frac{1}{2}E(q)\omega, \tag{3}$$

where

$$E(q) = \begin{pmatrix} -q_v^T \\ q_v^\times + q_0 I_3 \end{pmatrix},$$

and I_3 denotes the 3×3 identity matrix. Here, the notation $q_v^\times$ denotes the skew symmetry matrix, i.e.,

$$x^\times = \begin{bmatrix} 0 & -x_3 & x_2 \\ x_3 & 0 & -x_1 \\ -x_2 & x_1 & 0 \end{bmatrix}, \quad \forall x \in \mathbb{R}^3.$$

In addition, the dynamic equation of spacecraft attitude is given by

$$J\dot{\omega} = -\omega^\times J\omega + \tau + d(t), \tag{4}$$

where

- $J = J^T$ is the positive definite inertia matrix,
- $\omega = [\omega_1, \omega_2, \omega_3]^T$ is the angular velocity vector,
- $\tau = [\tau_1, \tau_2, \tau_3]^T$ is the control torque vector,
- $d(t)$ denotes the unknown time-varying external disturbances.

Furthermore, we have $E^T(q_i)E(q_i) = I_3$.

2.3 Control objectives

Different from the existing finite-time attitude control algorithm, not only the finite-time attitude stabilization can be achieved but also the angular velocity constraint is guaranteed.

Definition 2.1 (*Finite-time stability* [38]) For a continuous nonlinear system

$$\dot{u} = u(p), \quad u(0) = 0, \quad u \in \mathbb{R}^n, \tag{5}$$

where $u(\cdot) : \mathbb{R}^n \to \mathbb{R}^n$ is a continuous vector function, if system (5) satisfies the conditions Lyapunov stable and finite time convergent, then we can say it is finite-time stable. It means that there exists a function $T(p(0))$ such that $\lim_{t \to T(p(0))} u(t) = 0$ with $u(t) \equiv 0, \forall t \geq T(p(0))$.

Definition 2.2 (*Homogeneity* [39]) Define dilation $(g_1, \ldots, g_n) \in \mathbb{R}^n$ with $g_i > 0, i = 1, \ldots, n$. The function $u(p)$ defined in (5) can be said to be homogeneous with degree $\varrho \in \mathbb{R}$ with respect to $(g_1, \ldots, g_n)$ provided that for any given $\varepsilon > 0$,

$$u_i(\varepsilon^{g_1}p_1, \ldots, \varepsilon^{g_n}p_n) = \varepsilon^{\varrho+g_i}u_i(p), i = 1, \ldots, n, \forall p \in \mathbb{R}^n, \tag{6}$$

where $\varrho > -\min\{g_i, i = 1, \ldots, n\}$.

2.4 Related lemmas

Lemma 2.1 [40, 41] *If homogeneous system (5) is globally asymptotically stable and*

$$\lim_{\varepsilon \to 0} \frac{\widehat{u}_i(\varepsilon^{g_1}p_1, \ldots, \varrho^{g_n}p_n)}{\varepsilon^{\varrho+g_i}} = 0, i = 1, 2, \ldots, n, \forall p \neq 0, \tag{7}$$

following system (8)

$$\dot{u} = u(p) + \widehat{u}(p), u(0) = \widehat{u}(0) = 0, p \in \mathbb{R}^n, \tag{8}$$

is also globally finite-time stable.

Lemma 2.2 [42] *For any* $\varsigma > 0, p \in \mathbb{R}$, $d|p|^{\varsigma+1}/dp = (\varsigma+1)\text{sig}^\varsigma(p), d[\text{sig}^{\varsigma+1}(p)]/dp = (\varsigma+1)|p|^\varsigma$.

3 Main results

4 Design of constrained finite-time attitude controller

4.1 Case 1: case of no external disturbance

Define matrix

$$G(q_v) = (q_v^\times + q_0 I_3), \tag{9}$$

substituting (9) into (3), it can be obtained the following relation

$$\dot{q}_v = \frac{1}{2}(q_v^\times + q_0 I_3)w = \frac{1}{2}G(q_v)w. \tag{10}$$

Theorem 4.1 *For attitude control systems (4) and (10), if the controller τ is designed as*

$$\tau = -k_1 G^T(q_v)\text{sig}^{\alpha_1}(q_v) - \frac{k_2 M^{1+\alpha_2}}{|M^{1+\alpha_2} - \chi(\omega)|}\text{sig}^{\alpha_2}(\omega), \tag{11}$$

where $k_1 > 0$, $k_2 > 0$, $0 < \alpha_1 < 1$, $\alpha_2 = 2\alpha_1/(1+\alpha_1)$, $\chi(\omega) = |\omega_1|^{1+\alpha_2} + |\omega_2|^{1+\alpha_2} + |\omega_3|^{1+\alpha_2}$, *then*

- $|\omega_i(t)| < M$ *for all time,*
- $(q_v, \omega) \to 0$ *in a finite time,*

Proof The proof contains three parts. □

4.1.1 First part: state boundedness

Choose the Lyapunov function:

$$W = \frac{2k_1}{1+\alpha_1}\Big(\sum_{j=1}^{3}|q_{v,j}|^{1+\alpha_1}\Big) + \frac{1}{2}\omega^T J\omega. \tag{12}$$

It follows from Lemma 2.2 that

$$\begin{aligned}\dot{W} &= 2k_1\sum_{j=1}^{3}\text{sig}^{\alpha_1}(q_{v,j})\dot{q}_{v,j} + \omega^T J\dot{\omega} \\ &= k_1\omega^T G^T(q_v)\text{sig}^{\alpha_1}(q_v) + \omega^T\Big(-\omega^\times J\omega + \tau\Big).\end{aligned} \tag{13}$$

Here, the term $\omega^\times J\omega$ can be cancelled based on the model structure feature. Based on the skew symmetry, one obtains that

$$\omega^T\omega^\times J\omega = 0, \tag{14}$$

which leads to

$$\begin{aligned}\dot{W} &= k_1\omega^T G^T(q_v)\text{sig}^{\alpha_1}(q_v) + \omega^T\tau \\ &= -k_2\frac{M^{1+\alpha_2}}{|M^{1+\alpha_2}-\chi(\omega)|}\omega^T\text{sig}^{\alpha_2}(\omega) \\ &\leq 0.\end{aligned} \tag{15}$$

Hence, the system state (q_v, ω) is always bounded.

4.1.2 Second part: velocity constraint

In this part, we will show that $|\omega_i(t)| < M, i = 1, 2, 3$, for all time. Construct the function:

$$U = \frac{1}{1+\alpha_2}\sum_{j=1}^{3}|\omega_j|^{1+\alpha_2} = \frac{1}{1+\alpha_2}\chi(\omega), \tag{16}$$

whose derivative is

$$\begin{aligned}\dot{U} &= \sum_{j=1}^{3}\text{sig}^{\alpha_2}(\omega_j)\dot{\omega}_j \\ &= \text{sig}^{\alpha_2}(\omega)^T J^{-1}\Big(-\omega^\times J\omega + \tau\Big).\end{aligned} \tag{17}$$

Under the proposed controller, one obtains that

$$\begin{aligned}\dot{U} &= \text{sig}^{\alpha_2}(\omega)^T J^{-1}\Big(-\omega^\times J\omega - k_1 G^T(q_v)\text{sig}^{\alpha_1}(q_v)\Big) \\ &\quad - \frac{k_2 M^{1+\alpha_2}}{|M^{1+\alpha_2}-\chi(\omega)|}\text{sig}^{\alpha_2}(\omega)^T J^{-1}\text{sig}^{\alpha_2}(\omega).\end{aligned} \tag{18}$$

Based on the first part's proof, the first term in (18) is bounded, i.e., there is a constant C_1 that makes

$$\Big|\text{sig}^{\alpha_2}(\omega)^T J^{-1}\Big(-\omega^\times J\omega - k_1 G^T(q_v)\text{sig}^{\alpha_1}(q_v)\Big)\Big| \leq C_1. \tag{19}$$

However, for the second term in (18), if $\chi(\omega(t)) \to M^{1+\alpha_2}$ then

$$-\frac{k_2 M^{1+\alpha_2}}{|M^{1+\alpha_2}-\chi(\omega)|}\text{sig}^{\alpha_2}(\omega)^T J^{-1}\text{sig}^{\alpha_2}(\omega) \to -\infty. \tag{20}$$

Next, a contradiction proof can be used to show that $\chi(\omega) = M^{1+\alpha_2}$ is impossible. Suppose there exists a time T^* such that $\chi(\omega(T^*)) = M^{1+\alpha_2}$. As a result, based on (19) and (20), before the time T^*, there exists a time interval $[T^{**}, T^*)$ such that

$$\chi(\omega(t)) < M^{1+\alpha_2} \text{ and } \dot{U}(t) \leq 0, \ \forall t \in [T^{**}, T^*). \tag{21}$$

In other words,

$$U(T^*) \leq U(T^{**}). \tag{22}$$

By the definition of U in (16), one further gets that

$$\chi(\omega(T^*)) \leq \chi(\omega(T^{**})) < M^{1+\alpha_2}, \tag{23}$$

which conflicts the previous assumption that $\chi(\omega(T^*)) = M^{1+\alpha_2}$.

Hence, the conclusion can be made that $\chi(\omega(t)) < M^{1+\alpha_2}$ and $|\omega_i(t)| < M, i = 1, 2, 3$ for any time t.

4.1.3 Third Part: finite-time stability

Substituting proposed controller (11) into (4) to obtain the closed-loop system which can be described as:

$$\begin{aligned}\dot{q}_v &= \frac{1}{2}(q_v^\times + q_0 I_3)w = \frac{1}{2}G(q_v)w, \\ J\dot{\omega} &= -\omega^\times J\omega - k_1 G^T(q_v)\text{sig}^{\alpha_1}(q_v) \\ &\quad - \frac{k_2 M^{1+\alpha_2}}{|M^{1+\alpha_2}-\chi(\omega)|}\text{sig}^{\alpha_2}(\omega).\end{aligned} \tag{24}$$

The finite-time stability of system (24) is proved in two steps.

Step 1 Asymptotically stable

Based on the proof procedure in first part, it can be concluded which $(q_v, \omega) \to 0$ as $t \to \infty$ follows from LaSalle's invariant principle [43].

Step 2 Locally finite-time stable

System (24) can be reformed as

$$\begin{aligned}\dot{q}_v &= \frac{1}{2}G(0)\omega + \phi_1(q_v, \omega), \\ J\dot{\omega} &= -k_1 G^T(0)\text{sig}^{\alpha_1}(q_v) - k_2\text{sig}^{\alpha_2}(\omega) + \phi_2(q_v, \omega),\end{aligned} \tag{25}$$

where

$$\phi_1(q_v, \omega) = \frac{1}{2}\Big(G(q_v) - G(0)\Big)\omega,$$

$$\phi_2(q_v, \omega) = -\omega^\times J\omega - k_1\Big(G^T(q_v) - G^T(0)\Big)\text{sig}^{\alpha_1}(q_v)$$
$$- \Big(\frac{k_2 M^{1+\alpha_2}}{|M^{1+\alpha_2} - \chi(\omega)|} - k_2\Big)\text{sig}^{\alpha_2}(\omega). \tag{26}$$

First, consider the nominal part of (25), i.e.,

$$\dot{q_v} = \frac{1}{2}G(0)\omega,$$
$$J\dot{\omega} = -k_1 G^T(0)\text{sig}^{\alpha_1}(q_v) - k_2\text{sig}^{\alpha_2}(\omega). \tag{27}$$

Construct Lyapunov function as

$$V = \frac{2k_1}{1+\alpha_1}\Big(\sum_{j=1}^{3} |q_{v,j}|^{1+\alpha_1}\Big) + \frac{1}{2}\omega^T J\omega. \tag{28}$$

By a calculation, we have

$$\dot{V} = 2k_1 \sum_{j=1}^{3} \text{sig}^{\alpha_1}(q_{v,j})\dot{q}_{v,j} + \omega^T J\dot{\omega}$$
$$= -k_2\omega^T\text{sig}^{\alpha_2}(\omega) \tag{29}$$
$$\leq 0.$$

As with the above proof, system (27) can be proved to be asymptotically stable. And by Definition 2.2, it can be proved that system (27) has a homogeneous of degree $k = (\alpha_1 - 1)/2 < 0$ with respect to the dilation $(\lambda_1, \lambda_1, \lambda_1, \lambda_2, \lambda_2, \lambda_2)$, where $\lambda_1 = 1, \lambda_2 = (1 + \alpha_1)/2$.

Based on the definition of $G(q_v)$, we know it is a continuously differentiable function. It can be obtained via the mean inequality that

$$G(\varepsilon^{\lambda_1}q_v) - G(0) = O(\varepsilon^{\lambda_1}q_v), \tag{30}$$

and

$$G^T(\varepsilon^{\lambda_1}q_v) - G^T(0) = O(\varepsilon^{\lambda_1}q_v). \tag{31}$$

Next, we prove that $\lim_{\varepsilon\to 0}\frac{\phi_i(\varepsilon^{\lambda_1}q_v, \varepsilon^{\lambda_2}\omega)}{\varepsilon^{\lambda_i+k}} = 0$, $i = 1, 2$, for all $(q_v, \omega) \neq 0$. According to the definition of function $\phi_1(q_v, \omega)$, we have

$$\lim_{\varepsilon\to 0}\frac{\phi_1(\varepsilon^{\lambda_1}q_v, \varepsilon^{\lambda_2}\omega)}{\varepsilon^{\lambda_1+k}}$$
$$= \lim_{\varepsilon\to 0}\frac{\frac{1}{2}\Big(G(\varepsilon^{\lambda_1}q_v) - G(0)\Big)\varepsilon^{\lambda_2}\omega}{\varepsilon^{\lambda_1+k}} \tag{32}$$
$$= O(\varepsilon^{\lambda_1}q_v)\varepsilon^{\lambda_2-\lambda_1-k}\omega.$$

Because $r_2 - r_1 - k = 0$, then

$$\lim_{\varepsilon\to 0}\frac{\phi_1(\varepsilon^{\lambda_1}\dot{q_v}, \varepsilon^{\lambda_2}\omega)}{\varepsilon^{\lambda_1+k}} = O(\varepsilon^{\lambda_1}q_v)\omega = 0 \tag{33}$$

Similarly, based on the definition of function $\phi_2(q_v, \omega)$, we have

$$\lim_{\varepsilon\to 0}\frac{\phi_2(\varepsilon^{\lambda_1}q_v, \varepsilon^{\lambda_2}\omega)}{\varepsilon^{\lambda_2+k}}$$
$$= \lim_{\varepsilon\to 0} -\varepsilon^{-\lambda_2-k}\Big[\omega^\times J\omega + k_1\Big(G^T(\varepsilon^{\lambda_1}q_v) - G^T(0)\Big)\text{sig}^{\alpha_1}(\varepsilon^{\lambda_1}q_v)$$
$$+ \Big(\frac{k_2 M^{1+\alpha_2}}{|M^{1+\alpha_2} - \chi(\omega)|} - k_2\Big)\text{sig}^{\alpha_2}(\varepsilon^{\lambda_2}\omega)\Big]$$
$$= -\lim_{\varepsilon\to 0}\Big(k_1 O(\varepsilon^{\lambda_1}q_v)\varepsilon^{\lambda_1\alpha_1-\lambda_2-k}\text{sig}^{\alpha_1}(q_v) + \varepsilon^{-\lambda_2-k}\omega^\times J\omega$$
$$+ \Big(\frac{k_2 M^{1+\alpha_2}}{|M^{1+\alpha_2} - \chi(\omega)|} - k_2\Big)\varepsilon^{\lambda_2\alpha_2-\lambda_2-k}\text{sig}^{\alpha_2}(\omega)\Big). \tag{34}$$

Obviously, $\lambda_1\alpha_1 - \lambda_2 - k = 0$, $\lambda_2\alpha_2 - \lambda_2 - k = 0$, then

$$\lim_{\varepsilon\to 0}\frac{\phi_2(\varepsilon^{\lambda_1}q_v, \varepsilon^{\lambda_2}\omega)}{\varepsilon^{r_1+k}} = 0 \tag{35}$$

Therefore, by Lemma 2.1, the local finite-time stability and the global finite-time stability of the closed-loop system can be guaranteed, i.e., $(q_v, \omega) \to 0$ in a finite time. □

Remark 4.1 Note that in Theorem 4.1, if the fractional powers in novel finite-time controller (11) are chosen to be 1, i.e., $\alpha_1 = \alpha_2 = 1$, then the control torque will reduce to PD with the angular velocity constrained, i.e.,

$$\tau = -k_1 G^T(q_v)q_v - \frac{k_2 M^2}{|M^2 - \chi(\omega)|}\omega. \tag{36}$$

In the simulation section, the dynamic performance of the proposed control strategy can be shown by comparison with traditional PD controller as well as improved PD controller.

4.2 Case 2: case of exist external disturbances

The external disturbance in system (4) d(t) is bounded. To deal with lump disturbance d(t), an RBF neural network is employed to estimate d(t) [44]. Assume that an optimal weight W^* satisfies

$$d(\cdot) = W^{*T}h_d(x) + \varepsilon_d, \tag{37}$$

where $x = [q_v, \omega]^T$ is the input, $h_d(x)$ is the radial basis function of the neural network, ε_d is the network approximation error, and $|\varepsilon_d| \leq \varepsilon_{Md}$ with a constant ε_{Md}. According to the model, the output of the neural network is

$$\hat{d}(x) = \hat{W}^T h_d(x), \tag{38}$$

where $\hat{W}$ is an estimate value of the ideal weight W^*. The disturbance estimation error is

$$\begin{aligned} d(\cdot) - \hat{d}(x) &= W^{*T} h_d(x) + \varepsilon_d - \hat{W}^T h_d(x) \\ &= (W^{*T} - \hat{W}^T) h_d(x) + \varepsilon_d \\ &= W^T h_d(x) + \varepsilon_d, \end{aligned} \tag{39}$$

where

$$W^T = W^{*T} - \hat{W}^T. \tag{40}$$

The radial basis function can be expressed as:

$$h_d(x) = \exp\left(-\frac{\|x - c_j\|^2}{2b_j^2}\right), \quad j = 1, 2, \ldots, n, \tag{41}$$

where c_j is the data center of radial basis function in the j-th neuron of the hidden layer, and b_j is the width of radial basis function in the j-th neuron of the hidden layer.

As a result, the finite-time controller based on RBF neural network is designed as follows.

Theorem 4.2 *For attitude control subsystem* (4) *of quadrotor aircraft in the presence of external disturbances, if the controller is designed as*

$$\begin{aligned} \tau = &-k_1 G^T(q_v) \mathrm{sig}^{\alpha_1}(q_v) - \frac{k_2 M^{1+\alpha_2}}{|M^{1+\alpha_2} - \chi(\omega)|} \mathrm{sig}^{\alpha_2}(\omega) \\ &- \hat{d} - k_3 \mathrm{sign}(J^T s), \end{aligned} \tag{42}$$

where

$$s = J\omega + \int_0^\mu f(q_v, \omega) d\mu, \tag{43}$$

$$f(q_v, \omega) = k_1 G^T(q_v) \mathrm{sig}^{\alpha_1}(q_v) + \frac{k_2 M^{1+\alpha_2}}{|M^{1+\alpha_2} - \chi(\omega)|} \mathrm{sig}^{\alpha_2}(\omega), \tag{44}$$

where the $\hat{d}$ is the output of RBF neural network given by (38), k_3 is an appropriate positive constant, the parameters $\alpha_i, k_i, i = 1, 2$ are the same as that of Theorem 4.1, then the attitude of aircraft can converge to the desired state in a finite time. □

Proof First, it needs to be proven that system (4) can reach the sliding surface in a finite time. Then, we prove that $|\omega_i(t)| < M$.

Choose the Lyapunov function:

$$U = \frac{1}{2} s^T J s, \tag{45}$$

whose derivative is:

$$\begin{aligned} \dot{U} &= s^T J \dot{s} \\ &= s^T J \left(J\dot{\omega} + f(q_v, \omega) \right) \\ &= s^T J \left(-\omega^\times J\omega + \tau + d(t) + f(q_v, \omega) \right) \\ &\leq s^T J \left(d(t) - \hat{d}_\Phi - k_3 \mathrm{sign}(J^T s) \right) \\ &= -s^T J \left(k_3 \mathrm{sign}(J^T s) - W^T h_d(x) - \varepsilon_d \right) \\ &\leq -|s^T J| \left(k_3 - W^T h_d(x) - \varepsilon_d \right). \end{aligned} \tag{46}$$

Since the Gaussian function $h_d(x)$ and the function W^T are bounded, the $W^T h_d(x) + \varepsilon_d$ is bounded. As a result, if the gain satisfies $k_3 \geq W^T h_d(x) - \varepsilon_d$, then

$$\begin{aligned} \dot{U} &\leq -|s^T J|\gamma = -\sqrt{s^T J J^T s}\gamma \\ &\leq -\sqrt{\min\{J_{11}, J_{22}, J_{33}\} s^T J s}\gamma \\ &= -\sqrt{2U}\varrho, \end{aligned} \tag{47}$$

where

$$\varrho = \sqrt{\min\{J_{11}, J_{22}, J_{33}\}}\gamma. \tag{48}$$

Clearly, the sliding mode state s will converge to 0 in a finite time and always stay there.

Once $s \equiv 0$, then $\dot{s} \equiv 0$. As a result, it follows from (59) that

$$J\dot{\omega} = -k_1 G^T(q_v) \mathrm{sig}^{\alpha_1}(q_v) - \frac{k_2 M^{1+\alpha_2}}{|M^{1+\alpha_2} - \chi(\omega)|} \mathrm{sig}^{\alpha_2}(\omega). \tag{49}$$

Using an almost same proof as that of Case 1, it can be proven that the attitude will be stabilized in a finite time.

For $|\omega_i(t)| < M$, we construct the function:

$$P = \frac{1}{1 + \alpha_2} \sum_{j=1}^3 |\omega_j|^{1+\alpha_2} = \frac{1}{1 + \alpha_2} \chi(\omega), \tag{50}$$

whose derivative is

$$\begin{aligned} \dot{P} &= \sum_{j=1}^3 \mathrm{sig}^{\alpha_2}(\omega_j) \dot{\omega}_j \\ &= \mathrm{sig}^{\alpha_2}(\omega)^T J^{-1} \left(-\omega^\times J\omega + \tau + d(t) \right). \end{aligned} \tag{51}$$

Under the proposed controller, one obtains that

$$\begin{aligned} \dot{P} = &\mathrm{sig}^{\alpha_2}(\omega)^T J^{-1} \Big(-\omega^\times J\omega - k_1 G^T(q_v) \mathrm{sig}^{\alpha_1}(q_v) \\ &+ W^T h_d(x) + \varepsilon_d - k_3 \mathrm{sign}(J^T s) \Big) \\ &- \frac{k_2 M^{1+\alpha_2}}{|M^{1+\alpha_2} - \chi(\omega)|} \mathrm{sig}^{\alpha_2}(\omega)^T J^{-1} \mathrm{sig}^{\alpha_2}(\omega). \end{aligned} \tag{52}$$

Since s is always bounded, then the first term in (52) is bounded, i.e., there is a constant C_1 that makes

Table 1 The moment of inertia for aircraft

Description parameter (kg·m²)	Parameters definition	Nominal values
J_{xx}	X-axis of the rotary inertia	0.0049
J_{yy}	Y-axis of the rotary inertia	0.0049
J_{zz}	Z-axis of the rotary inertia	0.0088

Table 2 Controllers' parameters

Controller	Gains
Finite-time controller with angular velocity constraint (FTAC)	$k_1 = 6.11, k_2 = 4.98, \alpha_1 = 0.5, M = 0.33$
PD controller with angular velocity constraint (PDAC)	$k_1 = 6.15, k_2 = 4.63, \alpha_1 = 1, M = 0.33$
PD controller (PD)	$k_1 = 6.12, k_2 = 4.63, \alpha_1 = 1$

$$\left| \mathrm{sig}^{\alpha_2}(\omega)^T J^{-1} \Big(-\omega^\times J\omega - k_1 G^T(q_v)\mathrm{sig}^{\alpha_1}(q_v) \right.$$
$$\left. + W^T h_d(x) + \varepsilon_d - k_3\mathrm{sign}(J^T s) \Big) \right| \le C_1. \tag{53}$$

However, for the second term, if $\chi(\omega(t)) \to M^{1+\alpha_2}$ then

$$-\frac{k_2 M^{1+\alpha_2}}{|M^{1+\alpha_2} - \chi(\omega)|}\mathrm{sig}^{\alpha_2}(\omega)^T J^{-1}\mathrm{sig}^{\alpha_2}(\omega) \to -\infty. \tag{54}$$

Next, a contradiction proof can be used to show that $\chi(\omega) = M^{1+\alpha_2}$ is impossible. Suppose there exists a time T^* such that $\chi(\omega(T^*)) = M^{1+\alpha_2}$. As a result, based on (53) and (54), before the time T^*, there exists a time interval (T^{**}, T^*) such that

$$\chi(\omega(t)) < M^{1+\alpha_2} \quad \text{and} \quad \dot{P}(t) \le 0, \quad \forall t \in (T^{**}, T^*). \tag{55}$$

In other words,

$$P(T^*) \le P(T^{**}). \tag{56}$$

By the definition of P in (50), one further gets that

$$\chi(\omega(T^*)) \le \chi(\omega(T^{**})) < M^{1+\alpha_2}, \tag{57}$$

which conflicts the previous assumption that $\chi(\omega(T^*)) = M^{1+\alpha_2}$.

Hence, the conclusion can be made that $\chi(\omega(t)) < M^{1+\alpha_2}$ and $|\omega_i(t)| < M, i = 1, 2, 3$ for any time t.

The proof is completed. □

Remark 4.2 Note that in Theorem 4.2, if the fractional powers in novel finite-time controller (42) are chosen to be 1, i.e., $\alpha_1 = \alpha_2 = 1$, then the control torque will reduce to PD control with the angular velocity constrained that can deal with external disturbance, i.e.,

$$\tau = -k_1 G^T(q_v)q_v - \frac{k_2 M^2}{|M^2 - \chi(\omega)|}\omega - \hat{d} - k_3\mathrm{sign}(J^T s), \tag{58}$$

where

$$s = J\omega + \int_0^\mu f(q_v, \omega)\mathrm{d}\mu, \tag{59}$$

$$f(q_v, \omega) = k_1 G^T(q_v)q_v + \frac{k_2 M^2}{|M^2 - \chi(\omega)|}\omega, \tag{60}$$

where the $\hat{d}$ is the output of RBF neural network given by (38), k_3 is an appropriate positive constant, the parameters $\alpha_i, k_i, i = 1, 2$ are the same as that of Theorem 4.1, then the attitude of aircraft can converge asymptotically to the desired state. Compared with (58), the dynamic performance of the proposed control strategy is better, which can make the system stable in a finite time.

5 Simulation results

To verify the proposed theoretical results in Theorems 4.1 and 4.2, some numerical simulations are given. Two cases will be considered in this section.

For the first case, it is assumed that there are no external disturbances. To demonstrate the advantages of the proposed controller, two control strategies will be used for comparison, i.e., PD controller, PD controller with angular velocity constraint. In the second case, we consider the existence of external disturbances, a finite-time controller based on the integral terminal sliding mode control theory and the RBF neural network is employed.

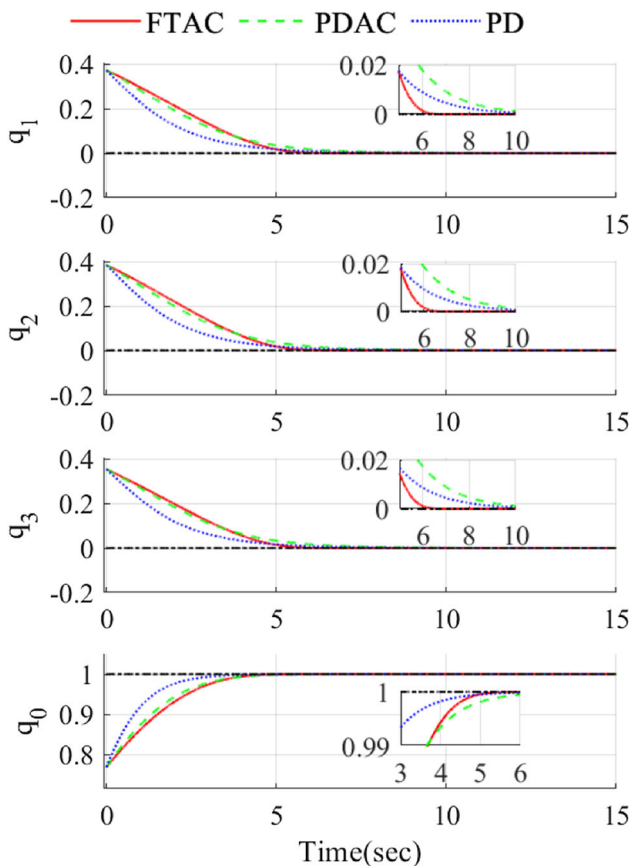The main parameters for the spacecraft are presented as Table 1 [45].

Fig. 1 The quaternion response curves for case 1

Fig. 2 The angular velocity response curves for case 1

For the simulation part, the initial state is selected as

$$(q_1(0), q_2(0), q_3(0), q_4(0), \omega_1(0), \omega_2(0), \omega_3(0))^T$$
$$= (0.7683, 0.371, 0.384, 0.353, -0.21, -0.23, -0.25)^T.$$

(61)

5.1 Case 1: case of no external disturbance

Table 2 lists the parameters of the controller.

As for the choose of controllers gains k_1 and k_2, by using the trial and error method, we do a number of simulations and then choose the better parameters for a satisfactory performance. Although the proposed finite-time algorithm contains the fractional power, it is not difficult to implement it based on a microcontroller (Pixhawk) with the C program. In order to compare the three controllers conveniently, the response curves of the three controllers are shown in the same figure. The quaternion response curve is shown in Fig. 1.

The angular velocity curves under three controller are shown in Fig. 2. In addition, in order to further illustrate that the proposed controller has better convergence speed, Table 3 is given, which compares the convergence time of
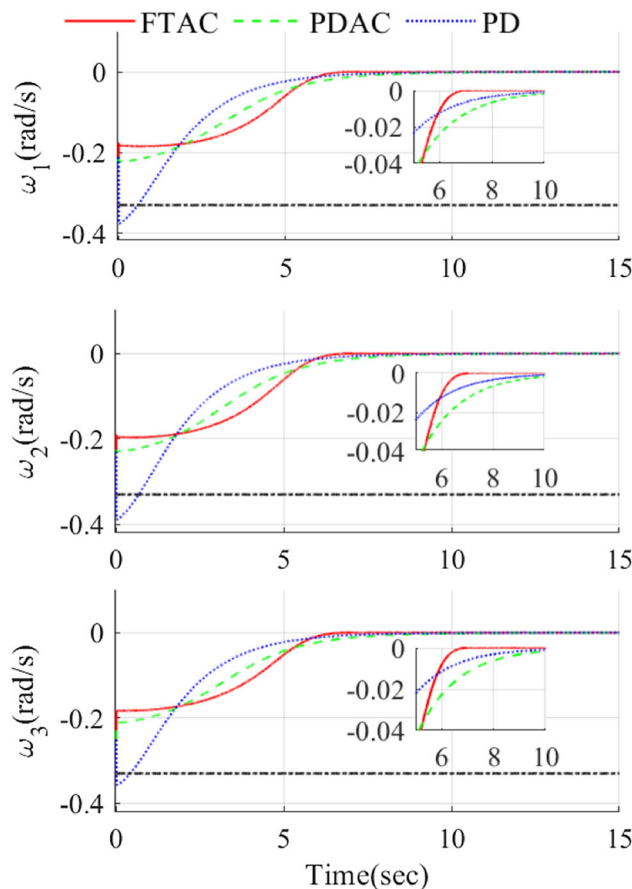
the three control methods. The symbol [bold] is used for less time to highlight the effect. The convergence time is defined as the time after which $|\omega_i| < 10^{-3}, i = 1, 2, 3$.

As shown in Fig. 2 and Table 3, PD control has a slower convergence rate than the proposed method, and the angular velocity exceeds the constraint scope. Although under the PD control with angular velocity constraint, angular velocity can be strictly constrained, its convergence rate is very slow. Compared with the first two control methods, finite-time control method with angular velocity constraint not only keeps the angular velocity strictly constrained, but also has the best convergence speed.

5.2 Case 2: case of exist external disturbances

In order to verify the above theoretical results, it is shown that the proposed controller has good robustness to external disturbances, and the external disturbances are selected as [46–48]

$$d_1(t) = 0.002 \sin(t + 5),$$
$$d_2(t) = 0.002 \cos(2t + 3),$$
$$d_3(t) = 0.003 \sin(3t + 2).$$

(62)
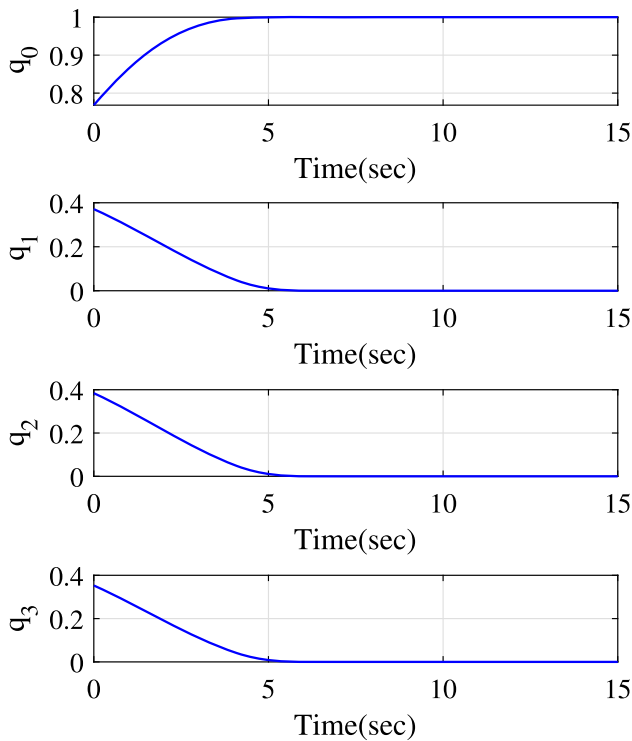
Table 3 The convergence time of the angular velocity under employed controllers

| Controller	Convergence time (s)		
	ω_1	ω_2	ω_3
Finite-time controller with angular velocity constraint (FTAC)	**8.860**	**8.877**	**8.765**
PD controller with angular velocity constraint (PDAC)	12.171	12.180	12.164
PD controller (PD)	9.715	9.674	9.678
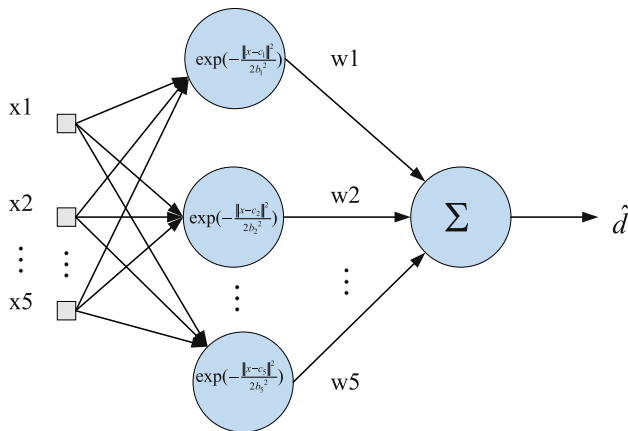
Fig. 3 The structure diagram of *RBF* neural network

Fig. 4 The quaternion response curves for case 2

The structure diagram of *RBF* neural network is shown in Fig. 3. The parameters for radial basis function (41) are selected as $c_j = [-1, -0.5, 0, 0.5, 1], bj = 1, j = $
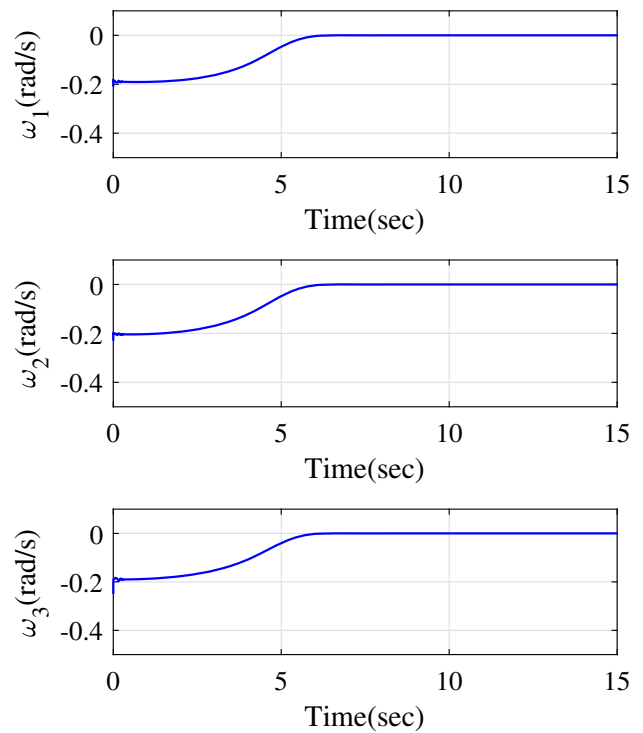
Fig. 5 The angular velocity response curves for case 2

$1, 2, 3, 4, 5$, the parameter for finite-time controller (42) is chosen as: $k_1 = 40, \alpha_1 = 0.5, k_2 = 55, \alpha_2 = 2/3, k_3 = 30$.

As shown in Fig. 4, it can be seen that the proposed finite-time controller based on RBF neural network is effective and has the capability to capture the disturbance $d(\cdot)$. Furthermore, from Fig. 5, it can be derived that by employing the proposed RBF-based neural network and terminal sliding mode control, the attitude stability control performance of aircraft with the angular velocity constraint and external disturbances can be further improved.

6 Conclusion

This paper has developed a finite-time attitude stabilization control method for a angular velocity constrained quadrotor aircraft in the presence of external disturbances. Firstly, a finite-time controller with angular velocity has been proposed to ensure the constrained angular velocity can be stabilized to the origin in a finite time. Then, a

finite-time controller based on sliding mode control theory and RBF neural network is proposed to solve the problem of exit external disturbances. At the end, simulation results have been given to verify the advantages of proposed control strategies.

References

1. Gui H, Vukovich G (2017) Finite-time angular velocity observers for rigid-body attitude tracking with bounded inputs. Int J Robust Nonlinear Control 27(1):15–38
2. Du H, Zhang J, Wu D, Zhu W, Li H, Chu Z (2020) Fixed-time attitude stabilization for a rigid spacecraft. ISA Trans 98:263–270
3. Cong Y, Du H, Jin Q (2020) Formation control for multi-quadrotor aircraft: connectivity preserving and collision avoidance. Int J Robust Nonlinear Control 30(6):2352–2366
4. Krstic M, Tsiotras P (1999) Inverse optimal stabilization of a rigid spacecraft. IEEE Trans Autom Control 44(5):1042–1049
5. Park Y (2005) Robust and optimal attitude stabilization of spacecraft with external disturbances. Aerosp Sci Technol 9(3):253–259
6. Gasagrandea D, Astolfi A, Parisini T (2008) Global asymptotic stabilization of the attitude and the angular rates of an underactuated non-symmetric rigid body. Automatica 44(7):1781–1789
7. Jiang B, Lu J, Liu Y, Cao J (2020) Periodic event-triggered adaptive control for attitude stabilization under input saturation. IEEE Trans Circuits Syst I(67):249–258
8. Cai M, Xiang Z (2018) Adaptive finite-time control of a class of non-triangular nonlinear systems with input saturation. Neural Comput Appl 29:565–576
9. Wang F, Hou M, Cao X (2019) Event-triggered backstepping control for attitude stabilization of spacecraft. J Frank Ins Eng Appl Math 356(16):9474–9501
10. Wang X, Li S, Chen M (2018) Composite backstepping consensus algorithms of leader-follower higher-order nonlinear multiagent systems subject to mismatched disturbances. IEEE Trans Cyber 48(6):1935–1946
11. Wang H, Mi C, Cao Z, Zheng J, Man Z, Jin X, Tang H (2020) Precise discrete-time steering control for robotic fish based on data-assisted technique and super-twisting-like algorithm. IEEE Trans Ind Electron 67(12):10587–10599
12. Zhang J, Wang H, Ma M, Yu M, Yazdani A, Chen L (2020) Active front steering-based electronic stability control for steer-by-wire vehicles via terminal sliding mode and extreme learning machine. IEEE Trans Veh Technol 69(12):14713–14726
13. Hu Y, Wang H, He S, Zheng J, Ping Z, Shao Ke, Cao Z, Man Z (2021) Adaptive tracking control of an electronic throttle valve based on recursive terminal sliding mode. IEEE Trans Veh Technol 70(1):251–262
14. Zhang J, Wang H, Zheng J, Cao Z, Man Z, Yu M, Chen L (2020) Adaptive sliding mode-based lateral stability control of steer-by-wire vehicles with experimental validations. IEEE Trans Veh Technol 69(9):9589–9600
15. Zhang J, Wang H, Cao Z, Zheng J, Yu M, Yazdani A, Shahnia F (2019) Fast nonsingular terminal sliding mode control for permanent magnet linear motor via ELM. Neural Comput Appl 32:14447–14457
16. Chen L, Wang H, Huang Y, Ping Z, Yu M, Ye M, Hu Y (2020) Robust hierarchical terminal sliding mode control of two-wheeled self-balancing vehicle using perturbation estimation. Mech Syst Sig Process. https://doi.org/10.1016/j.ymssp.2019.106584
17. Ding S, Liu L, Park J (2019) A novel adaptive nonsingular terminal sliding mode controller design and its application to active front steering system. Int J Robust Nonlinear Control 29(12):4250–4269
18. Hu Y, Wang H (2020) Robust tracking control for vehicle electronic throttle using adaptive dynamic sliding mode and extended state observer. Mech Syst Sig Process 135:1–18
19. Ning B, Han Q, Zuo Z (2019) Practical fixed-time consensus for integrator-type multi-agent systems: a time base generator approach. Automatica 105:406–414
20. Ding S, Park J, Chen C (2020) Second-order sliding mode controller design with output constraint. Automatica 112:1–8
21. Ning B, Han Q, Zuo Z, Jin J, Zheng J (2020) Collective behaviors of mobile robots beyond the nearest neighbor rules with switching topology. IEEE Trans Cybern 48(5):1577–1590
22. Wang K, Liu X, Jing Y (2020) Robust finite-time H_∞ congestion control for a class of AQM network systems. Neural Comput Appl. https://doi.org/10.1007/s00521-020-05168-z
23. Du H, Cheng Y, Wen G, Lv J (2021) Design and implementation of bounded finite-time control algorithm for speed regulation of permanent magnet synchronous motor. IEEE Trans Ind Electron 67(3):2417–2426
24. Hu Y, Wang H, Cao Z, Zheng J, Ping Z, Chen L, Jin X (2019) Extreme-learning-machine-based FNTSM control strategy for electronic throttle. Neural Comput Appl 32:14507–14518
25. Du H, Wen G, Wu D, Cheng Y, Lu J (2020) Distributed fixed-time consensus for nonlinear heterogeneous multi-agent systems. Automatica 113:1087–1097
26. Ding S, Mei K, Li S (2019) A new second-order sliding mode and its application to nonlinear constrained systems. IEEE Trans Automat Control 64(6):2545–2552
27. Wang X, Wang G, Li S (2020) Distributed finite-time optimization for integrator chain multiagent systems with disturbances. IEEE Trans Automat Control 65(12):5296–5311
28. Chen C, Sun Z (2020) Output feedback finite-time stabilization for high order planar systems with an output constraint. Automatica. https://doi.org/10.1016/j.automatica.2020.108843
29. Ding S, Park J, Tayebi Chen C (2020) Second-order sliding mode controller design with output constraint. Automatica. https://doi.org/10.1016/j.automatica.2019.108704
30. Zhu Z, Xia Y, Fu M (2011) Attitude stabilization of rigid spacecraft with finite-time convergence. Int J Robust Nonlinear Control 21(6):686–702
31. Du H, Li S (2012) Finite-time attitude stabilization for a spacecraft using homogeneous method. J Guid Control Dyn 35(3):740–748
32. Wie B, Lu J (1995) Feedback control logic for spacecraft eigenaxis rotations under slew rate and control constraints. J Guid Control Dyn 18(6):1372–1379
33. Shen Q, Yue C, Goh C, Wu B, Wang D (2018) Rigid-body attitude stabilization with attitude and angular rate constraints. Automatica 90:157–163
34. Sun L (2020) Adaptive fault-tolerant constrained control of cooperative spacecraft rendezvous and docking. IEEE Trans Ind Electron 67(4):3107–3115
35. Habibi H, Nohooji R, Howarda L, Simani S (2019) Fault-tolerant neuro adaptive constrained control of wind turbines for power regulation with uncertain wind speed variation. Energies 12:24. https://doi.org/10.3390/en12244712
36. Habibi H, Nohooji R, Howarda L (2019) Backstepping nussbaum gain dynamic surface control for a class of input and state constrained systems with actuator faults. Inf Sci 482:27–46
37. Shuster M (1993) A survey of attitude representations. J Astronaut Sci 41(4):439–517
38. Bhat S, Bernstein D (2000) Finite-time stability of continuous autonomous systems. SIAM J Control Opt 38(3):751–766

39. Bhat S, Bernstein D (1997) Finite-time stability of homogeneous systems. In: Proceedings of the American Control Conference. Albuquerque, NewMexico, 2513-2514

40. Hong Y, Huang J, Xu Y (2001) On an output feedback finite-time stabilization problem. IEEE Trans Automat Control 46(2):305–309

41. Hong Y, Xu Y, Huang J (2002) Finite-time control for robot manipulators. Syst Control Lett 46(4):185–200

42. Yu S, Yu X, Shirinzadeh B, Man Z (2005) Continuous finite-time control for robotic manipulators with terminal sliding mode. Automatica 41(11):1957–1964

43. Khalil H (2002) Nonlinear Systems. Prentice Hall, Upper Saddle River, NJ

44. Zhu W, Chen D, Du H, Wang X (2020) Position control for permanent magnet synchronous motor based on neural network and terminal sliding mode control. Trans Inst Meas Control 42(9):1632–1640

45. Tayebi A, McGilvray S (2006) Attitude stabilization of a VTOL quadrotor aircraft. EEE Trans Control Syst Technol 14(3):562–571

46. Zuo Z, Ru P (2014) Augmented L_1 adaptive tracking control of quad-rotor unmanned aircrafts. IEEE Trans Aerosp Electron Syst 50(4):3090–3101

47. Zhao B, Xian B, Zhang Y, Zhang X (2015) Nonlinear robust adaptive tracking control of a quadrotor UAV via immersion and invariance methodology. IEEE Trans Ind Electron 62(5):2891–2902

48. Du H, Zhu W, Wen G, Duan Z, Lv J (2017) Distributed formation control of multiple quadrotor aircraft based on nonsmooth consensus algorithms. IEEE Trans Cybern 49(1):342–353